Journal of Organometallic Chemistry 884 (2019) 66–76

Contents lists available at ScienceDirect

Journal of Organometallic Chemistry

journal homepage: www.elsevier.com/locate/jorganchem

Dinuclear and mononuclear oxorhenium(V) complexes chelated with the *S,O* bidentate thiourea ligand: Synthesis, crystal structure and catalytic activity

Suleyman Bozkurt, Ilkay Gumus*, Hakan Arslan

Department of Chemistry, Faculty of Arts and Science, Mersin University, Mersin, TR, 33343, Turkey

ARTICLE INFO

Article history:
Received 20 November 2018
Received in revised form
19 January 2019
Accepted 21 January 2019
Available online 28 January 2019

Keywords:
Oxorhenium(V) complexes
Thiourea ligands
Crystal structure
Catalyst
Sulfoxidation

ABSTRACT

N-(Diethylcarbamothioyl)-4-methylbenzamide ligand (HL) was prepared by subsequent reactions of *p*-toluoyl chloride with potassium thiocyanate and di-*n*-ethylamine, and used as a bidentate ligand for synthesis of mononuclear and dinuclear oxorhenium(V) complexes. The general procedure of mononuclear complexes involves the reaction of $(n\text{-Bu}_4)[ReOCl_4]$ with the bidentate HL ligand in alcohol solution to generate complexes of the form *cis*-$[Re^{V}O(L\text{-}\kappa^2S,O)_2(D)]$ where D = -OMe, OEt or $O^{i}Pr$. The product isolated from the reaction was found to be dependent on the reaction conditions applied and solvents used in particular re-crystallization. The obtainment of dinuclear complex involves the reaction of $(n\text{-Bu}_4N)[ReOCl_4]$ with the ligand in $MeCN/H_2O$ solution or the re-crystallization of mononuclear complexes in CH_2Cl_2/MeCN mixture. All complexes were characterized by ^1H and ^{13}C NMR, FTIR spectroscopy and single crystal X-ray diffraction studies. The ligand exchange chemistry of mononuclear complexes and their conversion to μ-oxo dimeric complexes based on solvent used to extend the coordination ability of the thiourea derivative ligand were also examined by ^1H NMR spectroscopy. The obtained complexes furthermore tested for their ability to catalyze the oxidation of diphenyl sulfide. The effects of various factors, such as amounts of catalyst, oxidants and solvent have been also investigated. The dimeric complex *cis*-$[(L\text{-}\kappa^2S,O)_2Re^{V}ORe^{V}(L\text{-}\kappa^2S,O)_2]$, under the optimized reaction conditions displays good catalytic activity with high selectivity while all monomeric complexes lead to lower conversion with high selectivities.

1. Introduction

The coordination chemistry of rhenium in high oxidation states has attracted attention due to their great importance as oxidation catalysts and ability to transfer an oxygen atom to appropriate organic substrate [1–6]. Especially, they were employed as excellent an oxygen atom transfer catalysts for oxidation reactions such as the oxidation of alkenes, sulfides, ketones and pyridines to the corresponding epoxides, sulfoxides and pyridine *N*-oxides [3,7].

Recently, several new developments into the chemistry of high valent oxo-complexes of rhenium were reported [8–20]. Among the most interesting ones was the successful deoxygenation using various reductants of a variety of functional groups such as sulfoxides, aromatic nitro groups, *N*-oxides, epoxides and diols promoted by oxo-complexes in high oxidation states [8]. In addition, they can also be used as catalysts in the activation of X-H (X = Si, B, P and H) bonds and C-X bond forming reactions [9–17]. The high-oxidation state of these complexes are also stable. Therefore, the complexes used in the catalysis process allows the reaction to be carried out under "open-flask" conditions, without the need for rigorous exclusion of air and moisture [18,19].

Recently, many studies have been reported the synthesis and crystal structure of a novel oxorhenium(V) complexes with various ligand systems in order to use as homogeneous catalysts for the oxidation of sulfides. Because sulfoxides are applied as catalysts, reagents, final products and especially as synthetic intermediates in the synthesis of biological and medicinal materials [20–23]. However, to the best of our knowledge no report is available in the literature with the oxorhenium(V) complexes of thiourea derivative ligands for the selective oxidation of sulfides. Therefore in this paper, we describe the syntheses of oxorhenium(V) complexes

* Corresponding author.
E-mail addresses: slymnbzkrt91@gmail.com (S. Bozkurt), ilkay.gumus@mersin.edu.tr (I. Gumus), hakan.arslan@mersin.edu.tr (H. Arslan).

https://doi.org/10.1016/j.jorganchem.2019.01.015
0022-328X/

using a *O*, *S*-coordinating thiourea derivative ligand. The structure of the complexes was characterized using NMR and FTIR spectroscopic techniques. Molecular structure of complexes was also investigated by X-ray single crystal diffraction study. The synthesized complexes has been evaluated as homogeneous catalyst for the oxidation of diphenyl sulfide to sulfoxide. Moreover, the oxidation of diphenyl sulfide was studied in more detail to optimize the reaction variables such as the amount of catalyst, oxidant molar ratio, reaction time and used solvent.

2. Result and discussion

2.1. Synthesis and characterization of mono- and di-nuclear complexes

Initially, the mononuclear oxorhenium complex **1**, *cis*-[$Re^{V}O(L^{2}$-$\kappa^{2}S,O)_2(OMe)$] (L is the deprotonated form of the ligand), was synthesized in good yields by refluxing (n-Bu_4N)[$ReOCl_4$] in MeOH with the chelating HL ligand and 2.2 equiv. of Et_3N as a proton scavenger and crystallized from an CH_2Cl_2:MeOH mixture (1:5, v:v). The formation of this type complex with axially coordinated methoxy ligand is a common feature of the chemistry of oxorhenium(V) compounds and has also been observed for thiourea derivative chelates of this metal (Scheme 1) [5,24–26]. The methoxy ligand is labile in the complex **1** and when CH_2Cl_2 solution of this complex was treated (re-crystallization) with different alcohols acting as Lewis base (EtOH and ^{i}PrOH). On the other hand, when the reaction between Re(V) and ligand precursor was carried out in desired different alcohol solutions, the corresponding alkoxy groups (-OEt or -O^{i}Pr) are coordinated to the metal center (Scheme 1) and so, complexes **2** and **3** were obtained.

The present of the methoxy, ethoxy and propoxy moieties coordinated as a donor to the monomeric complexes were confirmed by ^{1}H NMR. In the ^{1}H NMR spectrum of complex **1**, proton signals of the O–CH_3 group appeared at δ 3.49 ppm as singlet while the signals of the O–CH_2– and CH_2–CH_3 groups of complex **2** appeared at δ 3.49 ppm as quarted and at δ 0.65 ppm as triplet, respectively. The O–CH– and CH-(CH_3)$_2$ proton signals of the propoxy group in complex **3** appeared at δ 4.01–3.94 ppm as multiplet (overlaps with –CH_2– groups from the L ligand) and at δ 0.65 ppm as doublet, respectively. The signals appearing for these groups in the ^{1}H NMR spectra of monomeric complexes is not detected in the dimeric complex which supports coordination with the μ-oxo bridge. As a result, we can say that the ^{1}H NMR spectra of the mononuclear complexes **1**–**3** are consistent with the coordination of the methoxy, ethoxy and propoxy groups *trans* to the Re(V) oxo ligand, respectively. Unlike the alkoxy groups, the spectra of complexes **1**–**3** are rather similar, *i.e.* the methyl groups are seen as two separate triplet peaks at δ ~1.40 and 1.25 ppm, and the ethyl group signals for the ligand are seen as at δ ~4 ppm.

On the other hand, when the reaction between Re(V) and ligand precursor HL was carried out in MeCN:H_2O mixture in the absence of a proton scavenger, dinuclear complex **4** was obtained and crystallized from an CH_2Cl_2:MeCN mixture (1:5, v:v) as dark green cubic crystals. The dinuclear complex can also obtain from re-crystallized in CH_2Cl_2:MeCN mixture of mononuclear complexes. Similar conversion to dinuclear complex of mononuclear complexes occurs in MeCN, CH_2Cl_2, $CHCl_3$ and DMSO (especially in the presence of water) due to formation of an intermediate hydroxo species with the loss of the alkoxy groups [26,27].

We monitored conversion to the dinuclear complex **4** of mononuclear complex **1** in $CDCl_3$ by ^{1}H NMR (Fig. 1). The stack ^{1}H NMR spectra were measured at intervals of 20 min for 7 h, as shown in Fig. 1. The conversion can be easily distinguished based on ^{1}H NMR chemical shifts in stack spectra. In the interval of 0–6 min after addition of the $CDCl_3$, a new peaks at δ 8.20 and 7.17 ppm (shown with green triangle) appear and the intensity of the signals at δ 8.37 and 7.27 ppm from complex **1** diminishes. The peaks from complex **1** shown with red triangle disappears completely after 4 h and indicates the completing of the conversion. In the first minutes of the addition of $CDCl_3$ to the monomeric complex are observed the red solution in the NMR tube while at the end of 7 h of monitoring the reaction progress, a green solution are observed in the NMR tube. As a result, the complex **1** slowly converts to its dimeric form which can be noticed upfield shift and growth of signals from the dinuclear species in the stack spectra. In conclusion, it can be said that the products formed in reactions between Re(V) and ligand precursor were found to depend on the reaction conditions and re-crystallization of monomeric complex. In that formation of mononuclear and dinuclear complexes can be easily adjusted.

Vibrational spectroscopy was used to determine the structure of synthesized complexes and to discuss the nature of metal-oxo bonding. The characteristic ν(Re=O) stretching bond for complexes **1**–**3** showed at ~950 cm^{-1} while for complex **4** showed at ~956 cm^{-1}. This stretching bond in complexes **1**–**3** was bathochromically shifted, as expected for complexes incorporating a linear O=Re-OMe unit [5,24]. This bathochromic shifts in ν(Re=O) stretching bond of complexes **1**–**3** indicates a weakening of the ν(Re=O) bond and is consistent with partial double bond character of the Re-alkoxy due to competition of the alkoxy group for π-bonding with the d_π orbitals of the metal. FT-IR spectrum of complex **4** is also shows additional a peak at 663 cm^{-1}, due to the ν(Re-

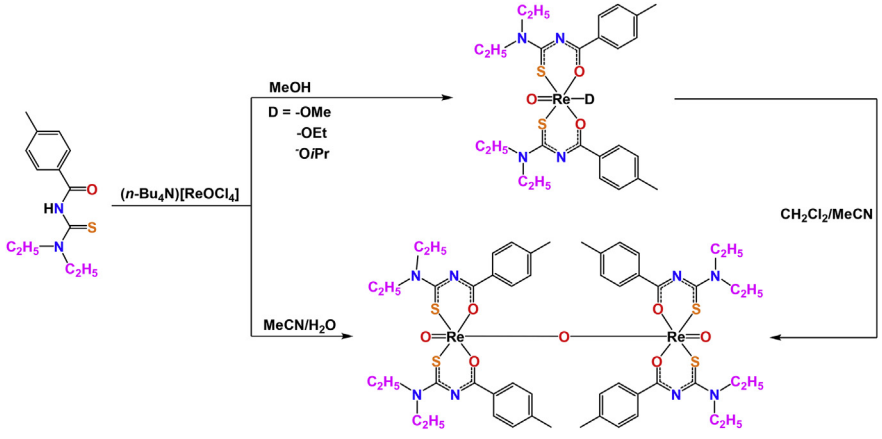

Scheme 1. Synthesis reaction of the prepared complexes.

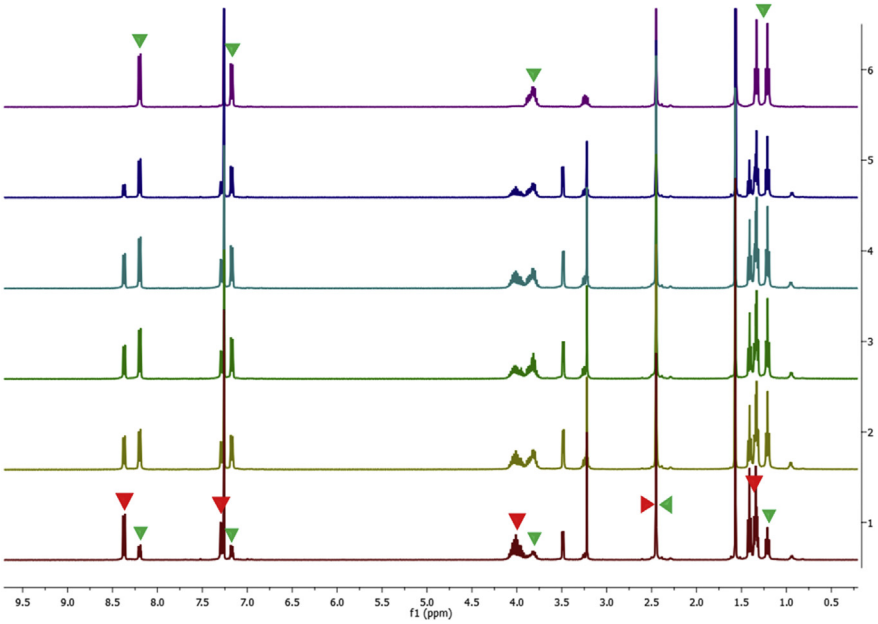

Fig. 1. The stack ^{1}H NMR spectra showing conversion to dimeric complex **4** (green triangles) of the monomeric complex **1** (red triangles). (For interpretation of the references to colour in this figure legend, the reader is referred to the Web version of this article.)

O–Re) stretch mode. The spectrum of all complexes displays the signature of carbonyl and thiocarbonyl stretch modes at 1525–1552 and 1292-1285 cm^{-1} due to the coordinated L^{-} moiety of ligand, respectively.

2.2. Molecular structures of the mono- and di-nuclear complexes

The molecular structure of all complexes was determined by a single-crystal X-ray diffraction technique and obtained results confirmed all spectroscopic data. Single crystals suitable for X-ray diffraction analyses of complexes **1**–**4** were obtained by diffusion of MeOH, EtOH, ^{i}PrOH and MeCN into the concentrated CH_2Cl_2 solutions of related complex, respectively. The complexes crystallize in monoclinic $P2_1/c$ space group with $Z = 4$ (complex **1**), in monoclinic space group $P2_1/n$ with $Z = 4$ (complex **2**), in triclinic space group *P*-1 with $Z = 2$ (complex **3**) and in triclinic space group *P*-1 with $Z = 1$ (complex **4**). The details of crystallographic data and structure refinement parameters are summarized in Table 1. The atom numbering for complexes is given in Fig. 2 with the relevant bond distances and angles collected in Table 2.

The molecular structures of complexes **1**–**3** are quite similar. They exhibit distorted octahedral geometry around the rhenium center *via* two chelating thiourea ligands coordinated in *cis* position to the oxo ligand and one alkoxy ligand in *trans* position to the oxo ligand, which form a linear O=Re-OR conformation (Figs. 2 and 3). The linear O=Re-OR conformation is common feature for rhenium(V) complexes due to considerable transfer of electron density from the Re=O bond into the Re-alkoxy bond [28].

The thiourea ligands bonded to rhenium ion forms two six-membered metallocycles, with the bite angles S(1)-Re(1)-O(1) and S(2)-Re(1)-O(2) being 92.66(6) and 92.39(5)° for complex **1**; 92.50(6) and 92.47(6)° for complex **2**; 92.25(2) and 91.40(5)° for complex **3**, respectively. On the other hand, the O=Re-O angles for complexes **1**–**3** are much below the ideal of 180° for an octahedral complex with 165.08(9), 164.26(10) and 168.24(9)°, respectively. The octahedral distortions in complexes result from the presence of multiple bonding terminal oxo ligand (the repulsion exerted by the oxo group on the equatorial ligands are increase) and bite angles of bidentate thiourea ligands [5].

The Re=O bond distances of complexes **1**–**3** are at 1.702(2), 1696(2) and 1.694(18) Å, respectively. These values verify an important contribution of π-bonding in total binding effect of rhenium-oxo ligand and consistent with a multiple Re=O bond. The Re-$O_{alkoxide}$ bond distances for complexes **1**–**3** are 1.901(19), 1.902(2) and 1.886(18) Å, respectively, and these values are similar to those reported in the literature [5,24,25]. The Re-$O_{thiourea}$ bond distances for complexes **1**–**3** are in the range of 2.116–2.122 Å, which is typical for these type complexes and fall within the range of similar Re(V) complexes [25]. The Re-$O_{thiourea}$ bond distances are in the range of 2.330–2.350 Å as seen Table 2. The Re-$S_{thiourea}$ bond lenghts in the all complexes are longer than Re-$O_{thiourea}$ bond lenghts. This effect can be understood in terms of Pearson's hard-soft acid-base theory. As hard Lewis acid Re(V) ion forms stronger bonds with oxygen rather than with the comparatively softer base sulfur donor.

The molecular structure of complex **4**, where two identical mononuclear structures are bonded to a bridging μ-oxo, is different from the complexes **1**–**3**. The complex **4** have a dimeric μ-oxo bridged form. The two rhenium atoms are six-coordinated in a distorted octahedral environment (Fig. 3). Each rhenium atom is ligated by two bidentate thiourea ligands, a terminal oxygen atom and a bridging μ-oxo atom. The chelating thiourea ligands bonded to rhenium forms two six membered rings, with the bite angles S1-Re1-O1 and S2-Re1-O2 being 92.06(6) and 91.90(6)°, respectively. The oxo ligands show the *cis* arrangement to two thiourea ligands. The oxo ligands and the μ-oxo bridged oxygen atom are found to be *trans* arrangement to each other. The Re–O3 bond distance of complex **4** is at 1.709(2) Å and Re-(μ-O) bond distance is at 1.916(13) Å. The average bond of Re–O3 is significantly shorter than that of Re-(μ-O), which could be attituded to the stronger competitive π-bonding of the rhenium with oxygen atom from bridged-oxo of Re–O–Re. At the same time, these values are in the expected range of similar complexes [29].

In the crystal structures of all complexes, the different packing of adjacent molecules is directed by a series of supramolecular contacts such as C–H···O and C–H···S, C–H···π and π···π

Table 1
Crystal data and details of the structure refinement for complexes **1**–**4**.

Parameter/Compound	*cis*-[$Re^{V}O(L\text{-}\kappa^2S,O)_2(OMe)$]	*cis*-[$Re^{V}O(L\text{-}\kappa^2S,O)_2(OEt)$]	*cis*-[$Re^{V}O(L\text{-}\kappa^2S,O)_2(O^{i}Pr)$]	*cis*-[$(L\text{-}\kappa^2S,O)_2Re^{V}ORe^{V}(L\text{-}\kappa^2S,O)_2$].$CH_3CN$
Empirical formula	$C_{27}H_{37}N_4O_4ReS_2$	$C_{28}H_{39}N_4O_4ReS_2$	$C_{29}H_{41}N_4O_4ReS_2$	$C_{60}H_{74}N_6O_7Re_2S_4$
Formula weight	731.92	745.95	759.98	1491.89
Temperature (K)	103.89	100	100.46	100.0
Crystal system	Monoclinic	Monoclinic	Triclinic	Triclinic
Space group	$P2_1/c$	$P2_1/n$	$P\text{-}1$	$P\text{-}1$
a (Å)	10.7152(6)	10.6120(6)	11.4474(6)	10.7353(5)
b (Å)	16.4177(10)	16.6399(9)	11.5719(7)	12.2370(6)
c (Å)	17.4548(10)	17.8201(8)	12.5244(8)	12.4351(7)
α (°)	90	90	76.184(5)	80.0696(16)
β (°)	106.258(2)	106.4628(16)	81.476(4)	84.9618(17)
γ (°)	90	90	75.817(4)	66.7474(15)
Volume ($Å^3$)	2947.8(3)	3017.7(3)	1554.87(17)	1478.05(13)
Z	4	4	2	1
ρ_{calc} (g/cm^3)	1.649	1.642	1.623	1.676
μ (mm^{-1})	4.302	4.204	4.082	4.290
F(000)	1464.0	1496.0	764.0	746.0
Crystal size (mm^3)	0.28 × 0.19 × 0.18	0.2 × 0.15 × 0.14	0.32 × 0.21 × 0.2	0.21 × 0.18 × 0.13
Radiation	MoKα (λ = 0.71073)	MoKα (λ = 0.71073)	MoKα (λ = 0.71073)	MoKα (λ = 0.71073)
2Θ range for data collection (°)	5.89 to 53.57	5.754 to 61.384	5.778 to 53.65	5.842 to 61.248
Index ranges	$-13 \le h \le 13$ $-20 \le k \le 20$ $-22 \le l \le 22$	$-15 \le h \le 15$ $-23 \le k \le 23$ $-25 \le l \le 20$	$-14 \le h \le 14$ $-14 \le k \le 14$ $-15 \le l \le 15$	$-15 \le h \le 15$ $-17 \le k \le 17$ $-17 \le l \le 17$
Reflections collected	60056	122439	47029	113476
Independent reflections	6286 [R_{int} = 0.0324, R_{sigma} = 0.0168]	9261 [R_{int} = 0.0821, R_{sigma} = 0.0313]	6613 [R_{int} = 0.0450, R_{sigma} = 0.0267]	9086 [R_{int} = 0.0734, R_{sigma} = 0.0291]
Data/restraints/parameters	6286/0/351	9261/0/359	6613/0/370	9086/0/350
Goodness-of-fit on F^2	1.179	1.059	1.077	1.114
Final R indexes [I ≥ 2σ (I)]	R_1 = 0.0218, wR_2 = 0.0457	R_1 = 0.0295, wR_2 = 0.0645	R_1 = 0.0209, wR_2 = 0.0406	R_1 = 0.0274, wR_2 = 0.0644
Final R indexes [all data]	R_1 = 0.0275, wR_2 = 0.0475	R_1 = 0.0436, wR_2 = 0.0698	R_1 = 0.0256, wR_2 = 0.0418	R_1 = 0.0331, wR_2 = 0.0664
Largest diff. peak/hole (e. $Å^{-3}$)	2.18/-1.06	3.62/-2.19	1.88/-0.91	2.06/-2.09

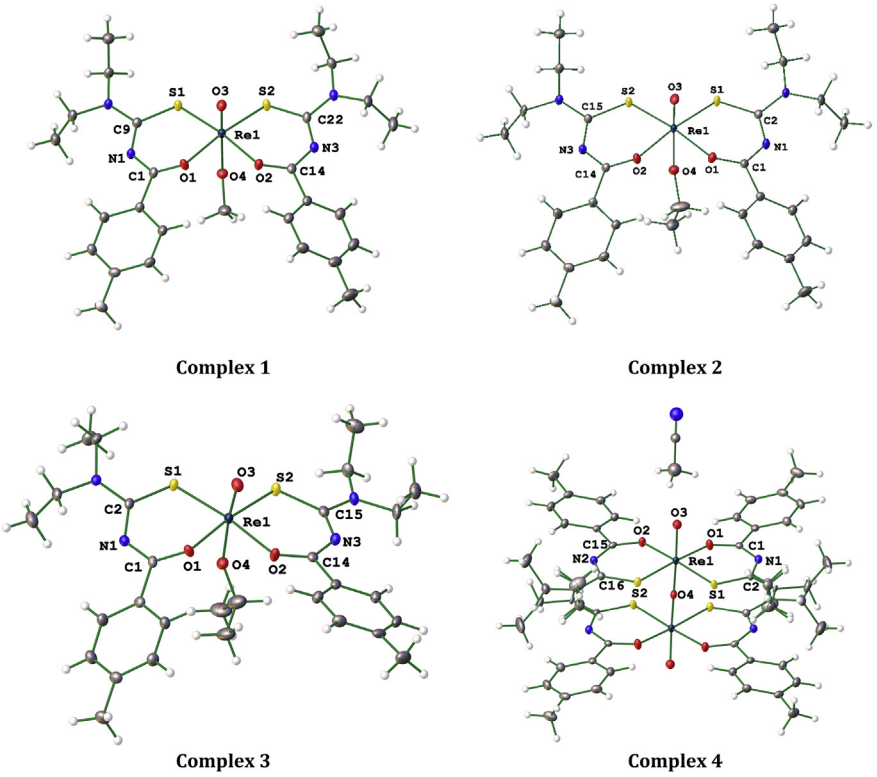

Fig. 2. Molecular structure of the prepared complexes **1**–**4**.

interactions contributing to the overall structural robustness. In complexes **1** and **2**, C–H···O, C–H···S and C–H···π interactions are dominate. In both complexes, the oxygen atom of oxo ligand acts as a multiple proton acceptor. The intermolecular C–H···O interaction in complex **1** occurs between oxo ligand oxygen atom as an acceptor and hydrogen atom of diethylamine part as a donor while the C–H···O interaction in complex **2** occurs between oxo ligand oxygen atom as an acceptor and hydrogen atoms of *p*-toluoyl

Table 2
Selected bond lengths and angles of complexes **1**–**4**.

Atom	Atom	Length (Å)	Atom	Atom	Atom	Angle (°)
Complex 1						
Re1	S1	2.3327(7)	S2	Re1	S1	91.38(2)
Re1	S2	2.3300(7)	O1	Re1	S1	92.66(6)
Re1	O1	2.1175(19)	O1	Re1	S2	173.23(6)
Re1	O2	2.1160(19)	O2	Re1	S1	172.91(6)
Re1	O3	1.702(2)	O3	Re1	O2	86.71(9)
Re1	O4	1.9005(19)	O3	Re1	O4	165.08(9)
S1	C9	1.763(3)	O4	Re1	S1	92.01(6)
O1	C1	1.272(3)	O4	Re1	S2	92.32(6)
N1	C1	1.324(4)	O2	Re1	S2	92.39(5)
N1	C9	1.349(4)	O2	Re1	O1	83.03(7)
N2	C9	1.330(4)	O3	Re1	S1	98.73(7)
Complex 2						
Re1	S2	2.3299(7)	S2	Re1	S1	90.63(2)
Re1	S1	2.3382(7)	O4	Re1	S2	92.45(6)
Re1	O4	1.901(2)	O4	Re1	S1	92.16(6)
Re1	O1	2.1196(19)	O4	Re1	O1	81.32(8)
Re1	O2	2.1223(19)	O4	Re1	O2	81.86(8)
Re1	O3	1.696(2)	O1	Re1	S2	173.12(6)
S1	C2	1.763(3)	O1	Re1	S1	92.50(6)
O4	C27	1.409(4)	O1	Re1	O2	83.81(8)
O1	C1	1.280(3)	O2	Re1	S2	92.47(6)
N3	C15	1.345(3)	O2	Re1	S1	173.37(6)
N3	C14	1.323(3)	O3	Re1	S2	99.37(7)
N1	C1	1.322(4)	O3	Re1	S1	98.03(7)
N1	C2	1.347(4)	O3	Re1	O4	164.26(10)
Complex 3						
Re1	S1	2.3449(6)	S1	Re1	S2	92.25(2)
Re1	S2	2.3506(7)	O1	Re1	S1	91.53(5)
Re1	O1	2.1227(17)	O1	Re1	S2	173.47(5)
Re1	O2	2.1179(17)	O2	Re1	S1	173.24(5)
Re1	O3	1.6948(18)	O2	Re1	S2	91.40(5)
Re1	O4	1.8863(18)	O2	Re1	O1	84.32(7)
S1	C2	1.759(3)	O3	Re1	S1	98.58(6)
O1	C1	1.280(3)	O3	Re1	S2	95.85(6)
N1	C1	1.328(3)	O3	Re1	O1	88.84(8)
N1	C2	1.348(3)	O3	Re1	O2	86.70(8)
N2	C2	1.336(3)	O3	Re1	O4	168.24(9)
Complex 4						
Re1	S2	2.3296(7)	S1	Re1	S2	89.65(2)
Re1	S1	2.3273(7)	O2	Re1	S2	91.90(6)
Re1	O2	2.1153(19)	O2	Re1	S1	174.61(6)
Re1	O3	1.709(2)	O3	Re1	S2	97.51(8)
Re1	O4	1.91633(13)	O3	Re1	S1	98.17(7)
Re1	O1	2.104(2)	O3	Re1	O2	86.75(9)
S1	C2	1.758(3)	O3	Re1	O4	164.50(7)
O4	Re1[1]	1.91637(13)	O3	Re1	O1	87.82(10)
O1	C1	1.270(3)	O4	Re1	S2	92.563(19)
C26	C25	1.522(5)	O4	Re1	S1	93.616(19)
N2	C15	1.328(4)	O4	Re1	O2	81.16(6)
N2	C16	1.344(3)	O4	Re1	O1	81.83(6)

part as a donor. The C–H···π interaction of complexes **1** and **2** consists between different donor and acceptor atoms as seen in Fig. 4. In the complex **1**, the C–H···π interaction occurs between Re-OCNCS chelate ring and hydrogen atom of diethylamine while in the complex **2** this interaction occur between *p*-toluoyl ring and hydrogen atom of *p*-toluoyl part.

Similarly in complex **3**, C–H···O and C–H···π intermolecular interactions occur. Unlike complexes **1** and **2**, in complex **3** the intermolecular C–H···O interaction consists between carbonyl oxygen atom of thiourea ligand and hydrogen atom of diethylamine while the C–H···π interactions occur between Re-SCNCO chelate ring acting as acceptor and hydrogen atoms of diethylamine part as seen in Fig. 5. For this reason, complex **3** has different crystal packing diagram. Unlike monomeric complexes, in the crystal structure of dimeric complex **4** reveals π···π stacking interactions involving the *p*-toluoyl rings of two adjacent molecules. These π···π stacking interactions help to connect neighboring molecules forming an interesting supramolecular framework. Intra- and intermolecular hydrogen bonds and geometrical parameters of C–H···π and π···π interactions for complexes **1**–**4** are given Tables 3 and 4.

2.3. Catalytic activity

After the successful preparation of the complexes, their catalytic performances were evaluated for sulfoxidation reaction. Reactivity of the synthesized complexes in sulfoxidation reaction was studied using diphenylsulfide as an oxygen acceptor model substrate. Before starting the activity studies, the control experiments were carried out without any catalyst and considerable sulfoxide yield was not observed. Without catalyst, control reactions showed that <5% reaction (after 2 h) occurred between excess ^{t}BuOOH and sulfide under the conditions used. In addition, only sulfoxide product was formed.

We choosed complex **4** as catalyst precursor in the oxidation progress of diphenyl sulfide in order to assess the best reaction conditions. To achieve the maximum conversion, different reaction parameters such as catalyst loading, oxidant (hydrogen peroxide (H_2O_2) and *tert*-butyl hydroperoxide (^{t}BuOOH)) and co-solvent were optimized. The progress of the reactions was monitored by ^{1}H NMR. Variations in catalyst loading, oxidants, reaction times and solvents are summarized in Table 5.

Firstly, the catalytic activity was evaluated in terms of the influence of solvents used and the $CHCl_3$, CH_3CN, CH_2Cl_2, MeOH and ^{i}PrOH were selected as co-solvents. The complex 4 exhibited a remarkable solubility in $CHCl_3$ and $CHCl_3$ at room temperature while it dissolved after the addition of oxidant in CH_3CN, MeOH and ^{i}PrOH. Therefore, it can be said that the complex 4 acts as a homogeneous catalyst in the oxidation of diphenyl sulfide. The effect of the used solvent was studied by keeping the other reaction conditions constant i.e. 1 mmol of difenyl sulfide, 0.01 mmol of catalyst and 2 mmol of ^{t}BuOOH at 296 K. When $CHCl_3$ and CH_2Cl_2 is used as a solvent, after 1 h nearly identical conversions were obtained. In that, the change of the reaction solvent from $CHCl_3$ to

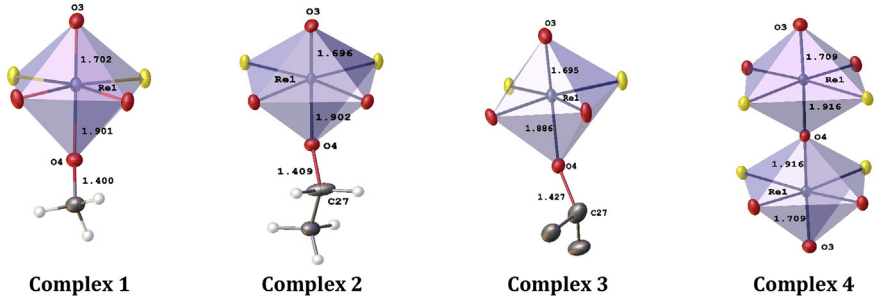

Complex 1 **Complex 2** **Complex 3** **Complex 4**

Fig. 3. The distorted coordination octahedra ReS_2O_4 in complexes **1**–**4**, in which the weakly bound sixth coordination site is shown at the bottom of each diagram. The displacement of the Re center from the median plane O1–O2–S1–S2 towards the apical oxo-oxygen O3 is apparent.

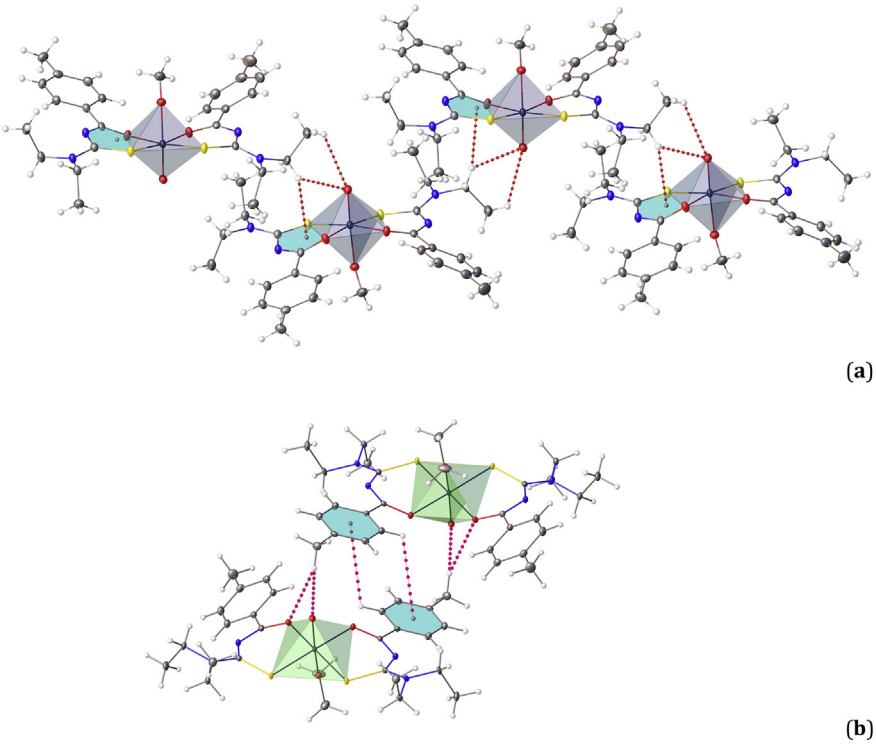

Fig. 4. The C–H···O and C–H···π intermolecular interactions between adjacent molecules in crystal lattice of complex **1** (a) and complex **2** (b).

CH_2Cl_2 does not affect the results (Table 5, Entry 1 and 2). Moderate conversions were observed in CH_3CN (Table 5, Entry 4). On the other hand, when MeOH and ^{i}PrOH is used, quite low conversions were observed (Table 5, Entry 5 and 6), this may be due to act as a competitive inhibitor for the attack of ^{t}BuOOH at the rhenium center of alcohol in reaction [30,31]. For this reason, we used $CHCl_3$ as the optimal co-solvent in the catalytic activity test. As a result, it can be said that the chlorinated solvents used in the catalytic activity test are the best co-solvent. So, all further experiments were performed in $CHCl_3$.

Secondly, the influence of oxidant used was also evaluated in the oxidation of diphenyl sulfide. The ^{t}BuOOH and H_2O_2 as oxidants were used. The effect of amount of oxidants H_2O_2 (aq. 34.5–35.5%) and ^{t}BuOOH (in 5.0–6.0 M in decane) was studied by varying their amount while other reaction conditions remained the same *i.e.* 1 mmol of difenyl sulfide, 1 mmol % of catalyst, and 1 mL of $CHCl_3$ at 296 K. For this goal, three different oxidant values *viz.* 1.0, 2.0 and 3.0 equiv. were chosen and reactions were carried out. Using 1.0, 2.0 and 3.0 mol equiv. of H_2O_2, the reaction was slower and conversion very low (*e.g.* after 1 h 8% of sulfoxide are obtained with 2.0 mol equiv. of H_2O_2). The reaction provided the best conversion when the oxidant was 2 mol equiv. of ^{t}BuOOH (*e.g.* after 1 h 58% of sulfoxide are obtained). Using a stoichiometric amount of 1.0 and 3.0 mol equiv. of ^{t}BuOOH the reaction was slower. It can be said that, the use of H_2O_2 as an oxidant in the oxidation of diphenyl sulfide did not yield significant amounts of the corresponding sulfoxite and 2.0 mol equiv. of ^{t}BuOOH was the more efficient oxidant reagent for this reaction.

The impact of catalyst amount was also evaluated for the sulfoxidation reaction and monitored the conversion by ^{1}H NMR study. Use of 0.01 mol of catalyst **4** with 2 equiv. of ^{t}BuOOH affords in good yield and perfect selectivity (*e.g.* after 1 and 2 h, 89 and 99% of sulfoxide are obtained, respectively, Table 5, entry 2 and 3). When the catalyst amount was reduced to 0.005 mol perfect selectivity is observed, but a longer reaction is required for the complete conversion of the diphenyl sulfide (*e.g.* after 1 and 2 h, 80 and 88% of sulfoxide are obtained, respectively, Table 5, entry 12 and 13).

We also evaluated the impact of 0.00250 mmol of catalyst **4** and after 2 h, 80% of sulfoxide are obtained (Table 5, entry 15). Using 0.00125 mmol of catalyst **4**, the reaction was slower and sulfoxide yield was significantly reduced (*e.g.* after 1 h, 40%). Fig. 6 shows stack ^{1}H NMR spectra taken at specific time intervals of this conversion. With addition of ^{t}BuOOH to pure diphenyl sulfide, the proton signals of diphenyl sulfide shift upfield possibly due to change in polarity and the new peaks at around δ 7.68 and 7.49 ppm which are correspond to diphenyl sulfoxide appears. In various time periods after addition of the ^{t}BuOOH, intensity of these new peaks increase and the intensity of the diphenyl sulfide signals diminish. After 240 min, the conversion rate is down and progressed by 2% increments in per 30 min period. This can be stated as follows: In the metal oxo complexes, likely oxidation mechanism includes the addition of ^{t}BuOOH a terminal M = O group, resulting in the formation of M = O···H and M···O$^{\alpha}$-O$^{\beta}$-^{t}Bu moieties. The α-O atom is then transferred to the substrate, producing the oxidized substrate under concomitant elimination of *tert*-butyl alcohol, yielding the initial complex (Fig. 7). The increased *tert*-butyl alcohol concentration in the solution slows down the conversion rate because *tert*-butyl alcohol can act as a competitive inhibitor for ^{t}BuOOH attack to metal center [30–33].

To sum up, it can be said that the amount of catalyst influences intensely the reaction ratio. When we use small amount of catalyst (0.00250 mmol), we found that we need more time to complete reaction for acceptable limits of yield. Also, when we use large amount of catalysts (0.01 mmol), we observed that we obtained the pure compound within very short reaction time such as 89% in 1 h. So, when we combine the amount of catalyst, reaction time and the cost of reaction, we can say that the best choice and optimum amount of catalyst is 0.005 mmol and we used this ratio in other tests.

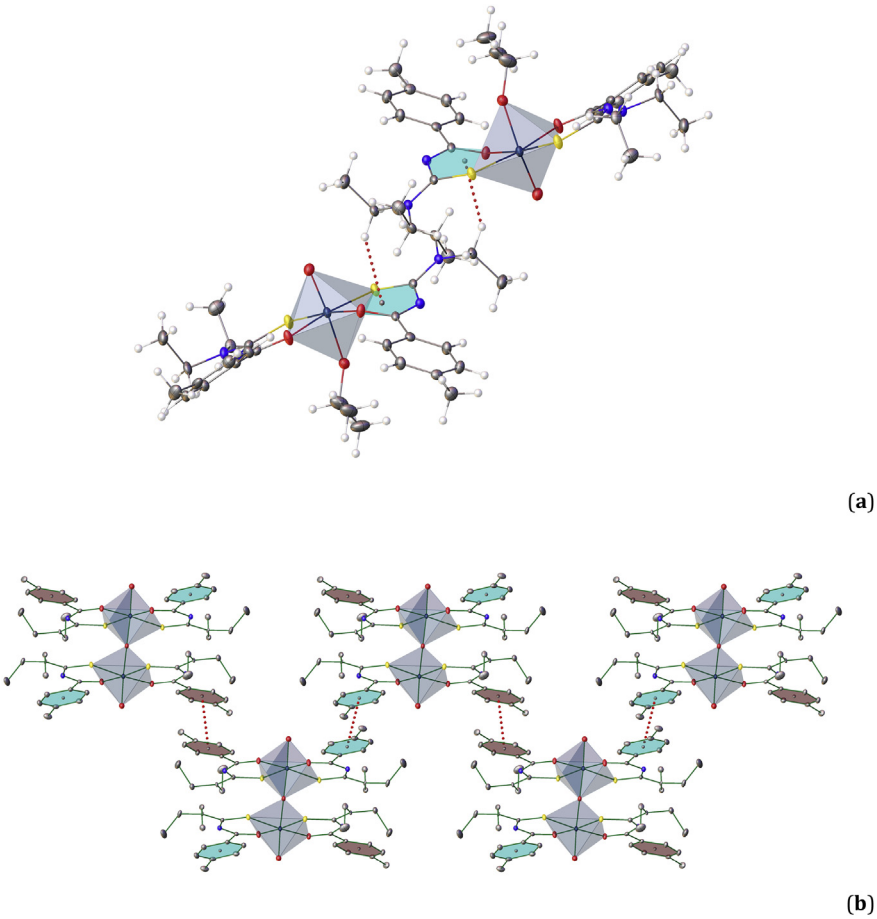

Fig. 5. (**a**) The C–H···π intermolecular interactions between two adjacent molecules in crystal lattice of complex **1** and (**b**) the π···π stacking interactions between adjacent molecules in crystal lattice of complex **2**.

Table 3
Intra- and inter-molecular hydrogen bonds for complexes **1**–**4** (Å, °)[a].

Complex	D-H···A	d(D-H)	d(H···A)	d(D···A)	∠(D-H···A)
1	C(10)-H(10A)···S(2) ^{i}	0.99	2.78	3.522(3)	132
	C(10)-H(10B)···S(1)	0.99	2.48	2.957(3)	109
	C(23)-H(23B)···O(3) ^{ii}	0.99	2.53	3.156(4)	121
	C(25)-H(25A)···S(2)	0.99	2.53	2.930(3)	104
	C(27)-H(27C)···O(2) ^{i}	0.98	2.55	3.057(4)	112
2	C(10)-H(10B)···O(3) ^{i}	0.99	2.57	3.192(4)	120
	C(12)-H(12A)···S(1)	0.99	2.53	2.944(3)	105
	C(23)-H(23A)···S(1) ^{ii}	0.99	2.83	3.624(3)	137
	C(23)-H(23B)···S(2)	0.99	2.47	2.958(3)	110
3	C(10)-H(10A)···S(1)	0.99	2.57	2.947(2)	103
	C(12)-H(12A)···O(1) ^{i}	0.99	2.57	3.523(3)	161
	C(23)-H(23A)···S(2)	0.99	2.49	2.938(3)	107
	C(26)-H(26B)···N(3)	0.98	2.57	3.068(4)	112
4 [b]	–	–	–	–	–

[a] Symmetry codes for compound **1**: *i* = -*x*, 1-*y*, -*z*, *ii* = -*x*, 1/2 + *y*, 1/2-*z*; for compound **2**: *i* = 2-*x*, 1-*y*, -*z*, *ii* = 5/2-*x*, −1/2 + *y*, 1/2-*z*; for compound **3**: *i* = 1-*x*, 2-*y*, 2-*z*.
[b] No interaction.

The other complexes **1**–**3** were tested under the above optimized reaction conditions for the maximum conversion of diphenyl sulfide (Table 6). The mononuclear oxo-complexes have very similar structures which coordinated by two molecules of the same bidentate *S,O* ligand. The only difference is found in the monodentate ancillary ligand, where complex **1** bears a methoxy, complex **2** an ethoxy and complex **3** a propoxy ligand. Although they have similar structures, differences in the activity are notable. The best activity among the monomeric complexes is complex **3** with 80% conversion after 1 h and after 2 h the conversion reached 90% with excellent selectivity. In the presence of catalyst **1**, the conversion reached 73% in 1 h and 90% in 2 h while in the presence of catalyst **2**, the conversion reached 78% in 1 h and 93% in 2 h. Overall, complex **1** performs slightly better than complex **2**.

All monomeric complexes exhibited excellent selectivity like dimeric complex **4** (Table 6). But, complexes **1** and **2** were not

Table 4
Geometrical parameters of C–H···π and π···π interactions for complexes **1**–**4** (Å, °)[a,b].

C–H···Cg(J)[c]	H···Cg	H-perp[d]	∠C–H···Cg	γ[e]	C···Cg[f]
Complex 1					
C(13) -H(13C)···Cg(4) [i]	2.82	2.82	142	3.94	3.642(4)
Complex 2					
C(26)-H(26C)···Cg(3) [i]	2.77	−2.77	139	1.85	3.568(4)
Complex 3					
C(27) -H(27)···Cg(2) [i]	2.87	−2.80	107	12.38	3.302(4)
Complex 4					
Cg(I)···Cg(J)	**Cg···Cg**	**Cg(I)-perp**	**Cg(J)-perp**	**γ[c]**	**-**
Cg(4)···Cg(4)[i]	3.99(11)	−3.4581(13)	−3.4581(13)	30.2	–

[a] Symmetry codes for complex **1**: $i = 1\text{-}x, -1/2 + y, 1/2\text{-}z$; for complex **2**: $i = 3/2\text{-}x, 1/2 + y, 1/2\text{-}z$; for complex **3**: $i = x, y, z$; for complex **4**: $i = 1\text{-}x, 1\text{-}y, 1\text{-}z$.
[b] The Cg(4) is gravity center of C15–C19 for complex **1**; the Cg(3) is gravity center of C3–C8 for complex **2**; the Cg(2) is gravity center of Re1-S2-C15-N3-C14-O2 for complex **3**; the Cg(4) is gravity center of C17–C22 for complex **4**.
[c] Center of gravity of ring J (Plane number above).
[d] Perpendicular distance of H to ring plane J.
[e] Angle between Cg-H vector and ring J normal.
[f] Distance between C-atom and the nearest carbon atom in the benzene ring.

Table 5
The effect of catalyst loading, oxidant and co-solvent in oxidation of diphenyl sulfide catalyzed by complex **4** [a].

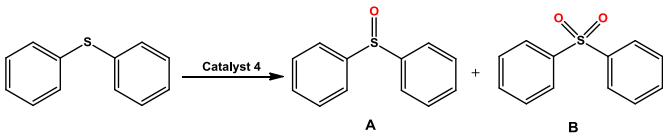

Entry	Catalyst (4)	Substrate	^{t}BuOOH	H_2O_2	Co-solvent	Time (h)	Conversion (%)	Selectivity A/B (%)	TON
1	0.01	1	2	–	CH_2Cl_2	1	86	100/0	86
2	**0.01**	1	**2**	–	**$CHCl_3$**	**1**	**89**	100/0	89
3	**0.01**	1	2	–	**$CHCl_3$**	**2**	**99**	100/0	99
4	0.01	1	2	–	CH_3CN	1	37	100/0	37
5	0.01	1	2	–	MeOH	1	10	100/0	10
6	0.01	1	2	-	^{i}PrOH	1	10	100/0	10
7	0.01	1	–	1	$CHCl_3$	1	8	100/0	8
8	0.01	1	–	2	$CHCl_3$	1	10	100/0	10
9	0.01	1	–	3	$CHCl_3$	1	11	100/0	11
10	0.01	1	1	–	$CHCl_3$	1	37	100/0	37
11	0.01	1	3	–	$CHCl_3$	1	70	100/0	70
12	**0.00500**	1	2	–	**$CHCl_3$**	**1**	**82**	100/0	164
13	**0.00500**	1	2	–	**$CHCl_3$**	**2**	**88**	100/0	176
14	0.00250	1	2	–	$CHCl_3$	1	69	100/0	276
15	**0.00250**	1	2	–	$CHCl_3$	2	**80**	100/0	320
16	**0.00250**	1	2	–	$CHCl_3$	3	**88**	100/0	352
17	0.00125	1	2	–	$CHCl_3$	1	40	100/0	320
18	0.00125	1	2	–	$CHCl_3$	2	53	100/0	424
19	0.00125	1	2	–	$CHCl_3$	3	64	100/0	512
20	0.00100	1	2	–	$CHCl_3$	1	36	100/0	360
21	0.00100	1	2	–	$CHCl_3$	2	47	100/0	470
22	0.00100	1	2	–	$CHCl_3$	3	56	100/0	560

[a] Reaction conditions: 296 K. Conversions were determined by ^{1}H NMR measurements after 1, 2 and 3 h. Complete selectivity towards the sulfoxidation was observed.

surpass the high catalytic activity of the complexes **3** and **4**. Previous studies have shown that in dimeric complexes a splitting across the oxo-bridge prior to ^{t}BuOOH coordination is necessary [34–37]. It has previously been explained in the literature that in comparative studies related monomeric and dimeric complexes exhibit similar activities pointing to a common monomeric catalytically active species. Therefore, monomeric and dimeric complexes are expected to have similar activity. However, the differences in the catalytic activities of the monomeric and dimeric complexes presented in this work are noticeable. This may be related to intermolecular interaction occurred between terminal oxo ligand and methyl hydrogen atom of adjacent molecule in complexes **1** and **2** (vide supra, Table 2 and Fig. 4, C23–H23B···O3=Re1 2.53 Å for complex **1** and C10–H10B···O3=Re1 2.57 Å for complex **2**). Because, this intermolecular interaction forms a barrier for the hydrogen bond (M = O···H) between the hydrogen atom of the ^{t}BuOOH and the terminal oxo ligand during the catalytic cycle.

3. Conclusion

Here, we presented a set of the monomeric and dimeric μ-oxo bridged rhenium(V) complexes ligated by bidentate the thiourea derivative ligand. The synthesized monomeric complexes have octahedral adducts with weakly bound a donor molecule D (OMe, OEt and O^{i}Pr). If the donor adducts are a volatile compound such as alcohol groups, the compound can be partially converted into a dimeric form, especially in the presence of water-containing

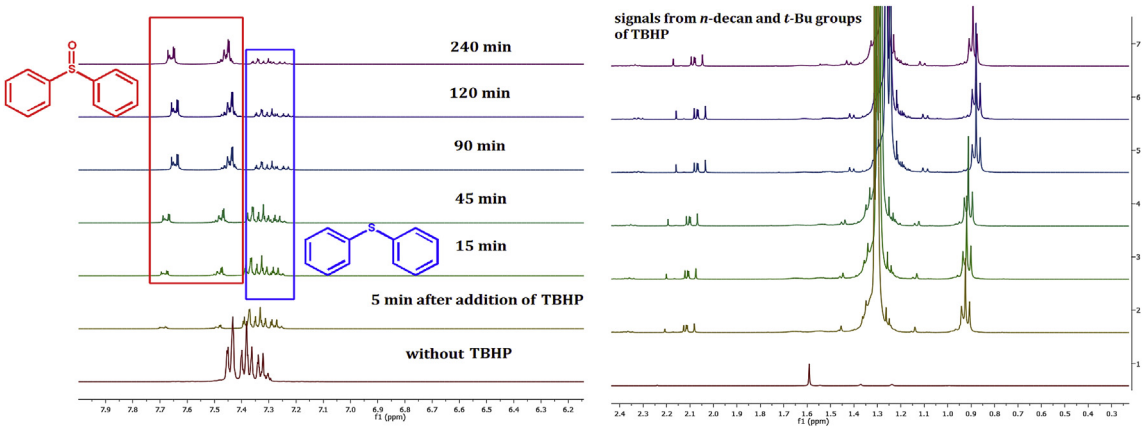

Fig. 6. Reaction progress monitored by ^{1}H NMR for the oxidation of diphenyl sulfide in $CDCl_3$ using complex **4** as catalyst.

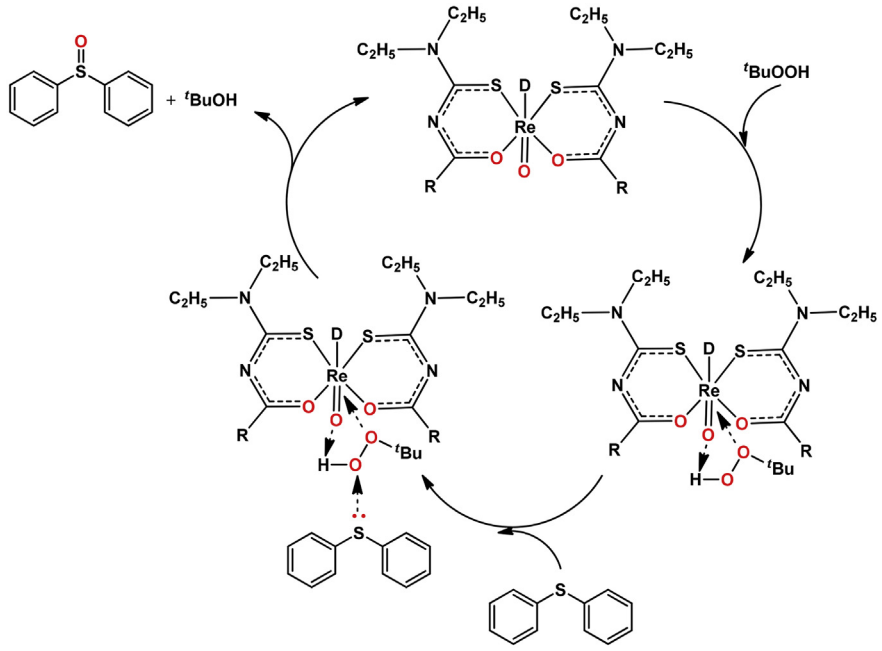

Fig. 7. Possible mechanism for the sulfoxidation reaction.

Table 6
The effect of complexes **1**–**3** as catalyst on oxidation of diphenyl sulfide[a].

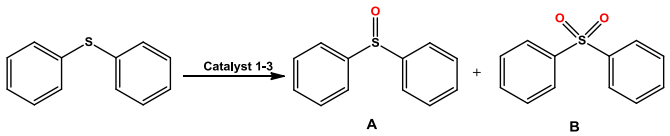

Entry	Catalyst	Time (h)	Conversion (%)	Selectivity A/B (%)	TON
1	**1**	1	73	100/0	146
2	**1**	2	86	100/0	172
3	**1**	3	99	100/0	198
4	**2**	1	78	100/0	156
5	**2**	2	90	100/0	180
6	**2**	3	99	100/0	198
7	**3**	1	80	100/0	160
8	**3**	2	99	100/0	198

[a] Reaction conditions: 0.005 mmol complexes **1**–**3**, 1 mmol diphenyl sulfide, 2 mmol ^{t}BuOOH (2 equiv.). Conversions were determined by ^{1}H NMR measurements after 1 and 2 h. Complete selectivity towards the sulfoxidation was observed.

solvents. X-ray diffraction analyses of complexes prove the existence of donor adducts for complexes **1**–**3** and prove a bridging O atom, which most probably occurs from water for complex **4**. The obtained all complexes act as catalysts in the oxidation of diphenyl sulfide using ^{t}BuOOH as oxidant. All complexes exhibited excellent selectivity, but complexes **3** and **4** has proven to be more active than the complexes **1** and **2**. In addition, although all the complexes show good catalytic activity in 1 h, the increase ratio in activity in 2 h decreased. These results revealed all complexes to be a highly active catalyst for diphenyl sulfide in comparison to complexes published by Wang and coworkers in 2002 [38].

4. Experimental

4.1. Materials

HL ligand was prepared as reported in the literature [39–45]. (n-Bu_4N)[$ReOCl_4$], diphenyl sulfide, 34.5–36.5% H_2O_2 and ^{t}BuOOH 5.0–6.0 M in n-decane used was purchased from Aldrich Chemical

Co. All of the solvents were purified by standard procedures.

4.2. Physical measurements

The NMR spectra were recorded in $CDCl_3$ solvent on Bruker Avance III 400 MHz NaNoBay FT-NMR spectrophotometer using tetramethylsilane as an internal standard. For infrared spectra, each compound was recorded in the range 400–4000 cm^{-1} on a Perkin Elmer Spectrum 100 series FT-IR/FIR/NIR Spectrometer Frontier, ATR Instrument.

The X-ray single crystal diffraction data were recorded on a Bruker APEX-II CCD diffractometer. A suitable crystal was selected and coated with Paratone oil and mounted onto a Nylon loop on a Bruker APEX-II CCD diffractometer. The crystal was kept at T = 100 K during data collection. The data were collected with MoKα (λ = 0.71073 Å) radiation for complexes **1**–**4** at a crystal-to-detector distance of 40 mm. Using Olex2 [46], the structure was solved with the Superflip [47–49] structure solution program, using the Charge Flipping solution method and refined by full-matrix least-squares techniques on F^2 using ShelXL [50] with refinement of F^2 against all reflections. Hydrogen atoms were constrained by difference maps and were refined isotropically, and all non-hydrogen atoms were refined anisotropically. The molecular structure plots were prepared using PLATON [51].

4.3. Synthesis of the complexes

4.3.1. Synthesis of cis-[$Re^{V}O(L\text{-}\kappa^2S,O)_2(OMe)$] (1)

The ligand (2 mmol, 2 equiv.) was dissolved in methanol (3 mL) and slowly added to a solution of (n-Bu_4N)[$ReOCl_4$] (1 mmol, 1 equiv.) in methanol (3 mL) and after 15 min, Et_3N (0.36 mL, 2 mmol, 2 equiv.) was added. The solution was stirred overnight at 50 °C. The resulting precipitate was filtered and washed twice with cold methanol (2 × 3 mL) (Scheme 1). The complex was crystallized from an CH_2Cl_2:MeOH mixture (1:5, *v*:*v*). Color: Red. Yield: 71%. Melting point: 179–181 °C. Elemental analysis (%): Calculated $C_{27}H_{37}N_4O_4ReS_2$: C, 44.31; H, 5.10; N, 7.65; Found: C, 43.29; H, 5.05; N, 7.55. FT-IR (ATR, ν, cm^{-1}): 2976, 2929 (C–H), 1579 (C–N), 1495 (C–O), 1247 (C=S), 948 (Re=O). ^{1}H NMR (400 MHz, $CDCl_3$, δ, ppm): 8.37 (dt, 4H, Ar–H), 7.28 (dt, 4H, Ar–H), 3.22 (s, 3H, OCH_3), 4.04-3.91 (m, 8H, CH_2), 2.45 (s, 6H, p-CH_3), 1.57 (t, 6H, CH_3), 1.33 (t, 6H, CH_3).

4.3.2. Synthesis of cis-[$Re^{V}O(L\text{-}\kappa^2S,O)_2(OEt)$] (2)

The ligand (2 mmol, 2 equiv.) was dissolved in methanol (3 mL) and slowly added to a solution of (n-Bu_4N)[$ReOCl_4$] (1 mmol, 1 equiv.) in methanol (3 mL) and after 15 min, Et_3N (0.36 mL, 2 mmol, 2 equiv.) was added. The solution was stirred over-night at 50 °C. The resulting precipitate was filtered and washed twice with cold methanol (2 × 3 mL) (Scheme 1). The complex was crystallized from an CH_2Cl_2:EtOH mixture (1:5, *v*:*v*). Color: Red. Yield: 70%. Melting point: 181–183 °C. Elemental analysis (%): Calculated $C_{28}H_{39}N_4O_4ReS_2$: C, 45.08; H, 5.27; N, 7.51; Found: C, 45.01; H, 5.18; N, 7.43. FT-IR (ATR, ν, cm^{-1}): 2976, 2929 (C–H), 1579 (C–N), 1495 (C–O), 1247 (C=S), 948 (Re=O). ^{1}H NMR (400 MHz, $CDCl_3$, δ, ppm): 8.35 (dt, 4H, Ar–H), 7.23 (dt, 4H, Ar–H), 4.01-3.94 (s, 8H, O–CH_2–CH_3), 3.50 (q, 2H, O–CH_2), 2.45 (s, 6H, p-CH_3), 1.57 (t, 6H, CH_3), 1.33 (t, 6H, CH_3), 0.65 (t, 3H, CH_2CH_3).

4.3.3. Synthesis of cis-[$Re^{V}O(L\text{-}\kappa^2S,O)_2(O^{i}Pr)$] (3)

The ligand (2 mmol, 2 equiv.) was dissolved in methanol (3 mL) and slowly added to a solution of (n-Bu_4N)[$ReOCl_4$] (1 mmol, 1 equiv.) in methanol (3 mL) and after 15 min, Et_3N (0.36 mL, 2 mmol, 2 equiv.) was added. The solution was stirred over-night at 50 °C. The resulting precipitate was filtered and washed twice with cold methanol (2 × 3 mL) (Scheme 1). The complex was crystallized from an CH_2Cl_2: ^{i}PrOH mixture (1:5, *v*:*v*). Color: Red. Yield: 72%. Melting point: 182–184 °C. Elemental analysis (%): Calculated $C_{29}H_{41}N_4O_4ReS_2$: C, 45.83; H, 5.44; N, 7.37; Found: C, 45.66; H, 5.38; N, 7.30. FT-IR (ATR, ν, cm^{-1}): 2968, 2932 (C–H), 1579 (C–N), 1495 (C–O), 1246 (C=S), 934 (Re=O). ^{1}H NMR (400 MHz, $CDCl_3$, δ, ppm): 8.34 (dt, 4H, Ar–H), 7.29 (dt, 4H, Ar–H), 4.06-3.98 (m, 8H+1H, CH_2+O–CH), 2.45 (s, 6H, p-CH_3), 1.40 (t, 6H, CH_3), 1.24 (t, 6H, CH_3), 0.65 (d, 6H, CH_3).

4.3.4. Synthesis of cis-[$(L\text{-}\kappa^2S,O)_2Re^{V}ORe^{V}(L\text{-}\kappa^2S,O)_2$].$CH_3CN$ (4)

The ligand (1 mmol, 1 equiv.) was dissolved in MeCN (3 mL) and slowly added to a solution of (n-Bu_4N)[$ReOCl_4$] (1 mmol, 1 equiv.) in acetonitrile (3 mL) and after 2 h, water was added to reaction mixture and the resulting green precipitate was filtered and washed twice with cold acetonitrile (2 × 3 mL). The complex was crystallized from an CH_2Cl_2: MeCN mixture (1:5, *v*:*v*) (Scheme 1). Color: Red. Yield: 70%. Melting Point: 197–199 °C. Elemental analysis (%): Calculated $C_{52}H_{68}N_8O_7Re_2S_4$: C, 44.05; H, 4.83; N, 7.90; Found: C, 43.99; H, 4.75; N, 7.84. FT-IR (ATR, ν, cm^{-1}): 2983, 2933 (C–H), 1580 (C–N), 1483 (C–O), 1245 (C=S), 942 (Re=O), 669 (O=Re-O–Re=O). ^{1}H NMR (400 MHz, $CDCl_3$, δ, ppm): 8.20 (dt, 8H, Ar–H), 7.17 (dt, 8H, Ar–H), 3.89-3.78 (m, 16H, CH_2), 2.45 (s, 12H, p-CH_3), 1.40 (t, 12H, CH_3), 1.21 (t, 12H, CH_3). ^{13}C NMR (100 MHz, $CDCl_3$, δ, ppm): 182.25 (C–S), 172.36 (C–O), 141.47 (C–Ar), 135.43 (C–Ar), 130.76 (C–Ar), 128.19 (C–Ar), 47.20 (C–N), 45.69 (C–N), 21.65 (CH_2), 13.40 (CH_3), 13.30 (CH_3).

4.4. Catalytic activity test

Overall, catalytic experiments were run in deuterated chloroform solutions and the reactions were monitored by ^{1}H NMR spectroscopy. Solutions of *tert*-butyl hydroperoxide and diphenyl sulfide were added in a 5 mm NMR tube. The catalyst was added and the reaction rates were estimated on the basis of the integrated intensities of substrate and product spectra.

Acknowledgements

This work was supported by the Mersin University Research Fund [Project No: 2017-1-TP2-2107]. This academic work was linguistically supported by the Mersin Technology Transfer Office Academic Writing Center of Mersin University.

Appendix A. Supplementary data

Supplementary data to this article can be found online at https://doi.org/10.1016/j.jorganchem.2019.01.015.

Disclosure statement

Conflict of interests

The authors declare that they have no conflict of interest.

Author contributions

All authors contributed equally to this work.

Ethical approval

All ethical guidelines have been adhered.

Sample availability

Samples of the compounds are available from the author.

References

[1] R. Sarkar, A. Hensa, K.K. Rajak, RSC Adv. 5 (2015) 15084–15095.
[2] S. Dinda, A. Genest, N. Rosch, ACS Catal. 5 (8) (2015) 4869–4880.
[3] S.C.A. Sousa, I. Cabritaa, A.C. Fernandes, Chem. Soc. Rev. 41 (2012) 5641–5653.
[4] R. Sarkar, P. Mondal, K.K. Rajak, Dalton Trans. 43 (2014) 2859–2877.
[5] B. Machura, M. Wolff, E. Benoist, J.A. Schachnerd, N.C. Mösch-Zanettid, Dalton Trans. 42 (2013) 8827–8837.
[6] J.A. Schachner, B. Terfassa, L.M. Peschel, N. Zwettler, F. Belaj, P. Cias, G. Gescheidt, N.C. Mösch-Zanetti, Inorg. Chem. 53 (24) (2014) 12918–12928.
[7] J.L. Smeltz, C.P. Lilly, P.D. Boyle, E.A. Ison, J. Am. Chem. Soc. 135 (2013) 9433–9441.
[8] L.M.D.R.S. Martins, A.J.L. Pombeiro, Inorg. Chim. Acta. 455 (2017) 390–397.
[9] S.C.A. Sousa, A.C. Fernandes, Coord. Chem. Rev. 284 (2015) 67–92.
[10] A.C. Fernandes, J.A. Fernandes, F.A. Almeida Paz, C.C. Romao, Dalton Trans. 47 (2008) 6686–6688.
[11] R.G. Noronha, P.J. Costa, C.C. Romao, M.J. Calhorda, A.C. Fernandes, Organometallics 28 (2009) 6206–6212.
[12] R.G. Noronha, C.C. Romao, A.C. Fernandes, Catal. Commun. 12 (2011) 337–340.
[13] P.M. Reis, P.J. Costa, C.C. Romão, J.A. Fernandes, M.J. Calhorda, B. Royo, Dalton Trans. 13 (2008) 1727–1733.
[14] S.C.A. Sousa, A.C. Fernandes, Adv. Synth. Catal. 352 (2010) 2218–2226.
[15] J.R. Bernardo, S.C.A. Sousa, P.R. Florindo, M. Wolff, B. Machura, A.C. Fernandes, Tetrahedron 69 (2013) 9145–9154.
[16] B.G. Das, P. Ghorai, Chem. Commun. 48 (2012) 8276–8278.
[17] B.G. Das, P. Ghorai, Org. Biomol. Chem. 11 (2013) 4379–4382.
[18] M.R. Luzung, F.D. Toste, J. Am. Chem. Soc. 125 (2003) 15760–15761.
[19] I. Gryca, B. Machura, L.S. Shulpina, G.B. Shulpin, Inorg. Chim. Acta. 455 (2017) 683–695.
[20] M.C. Carreno, Chem. Rev. 95 (1995) 1717–1760.
[21] B. Karimi, D. Zareyee, J. Iran. Chem. Soc. 5 (2008) 103–107.
[22] E.N. Prilezhaeva, Russ. Chem. Rev. 70 (2001) 897–920.
[23] B. Machura, M. Wolff, D. Tabak, J.A. Schachner, N.C. Mosch-Zanetti, Eur. J. Inorg. Chem. 23 (2012) 3764–3773.
[24] H. Braband, O. Blatt, U. Abram, Z. Anorg. Allg. Chem. 632 (2006) 2251–2255.
[25] N.H. Huy, U. Abram, Inorg. Chem. 46 (13) (2007) 5310–5319.
[26] L. Hansen, E. Alessio, M. Iwamoto, P.A. Marzilli, L.G. Marzilli, Inorg. Chim. Acta. 240 (1995) 413–417.
[27] N.P. Johnson, F.I.M. Taha, G. Wilkinson, J. Chem. Soc. (1964) 2614–2616.
[28] B. Machura, M. Wolff, I. Gryca, Coord. Chem. Rev. 275 (2014) 154–164.
[29] D.A. Rotsch, K.M. Reinig, E.M. Weis, A.B. Taylor, C.L. Barnesa, S.S. Jurisson, Dalton Trans. 42 (2013) 11614–11625.
[30] M.E. Judmaier, C.H. Sala, F. Belaj, M. Volpe, N.C. Mosch-Zanetti, New J. Chem. 37 (2013) 2139–2149.
[31] A. Al-Ajlouni, A.A. Valente, C.D. Nunes, M. Pillinger, A.M. Santos, J. Zhao, C.C. Romao, I.S. Goncalves, F.E. Kuhn, Eur. J. Inorg. Chem. (2005) 1716–1723.
[32] M. Jaccob, P. Comba, M. Maurer, P. Vadivelu, P. Venuvanalingam, Dalton Trans. 40 (2011) 11276–11281.
[33] K.L. Wong, Y.M. So, G.C. Wang, H.H.Y. Sung, I.D. Williams, W.H. Leung, Dalton Trans. 45 (2016) 8770–8776.
[34] S. Gago, P. Neves, B. Monteiro, M. Pessego, A.D. Lopes, A.A. Valente, F.A. Almeida Paz, M. Pillinger, J. Moreira, C.M. Silva, I.S. Gonçalves, Eur. J. Inorg. Chem. 2009 (2009) 4528–4537.
[35] J.M. Mitchell, N.S. Finney, J. Am. Chem. Soc. 123 (2001) 862–869.
[36] J.A. Brito, N. Saffon, M. Gomez, B. Royo, Curr. Inorg. Chem. 1 (2011) 131–139.
[37] J. Morlot, N. Uyttebroeck, D. Agustin, R. Poli, Chem. Cat. Chem. 5 (2013) 601–611.
[38] Y. Wang, G. Lente, J.H. Espenson, Inorg. Chem. 41 (5) (2002) 1272–1280.
[39] N. Ozpozan, T. Ozpozan, H. Arslan, N. Kulcu, Thermochim. Acta 336 (1999) 97–103.
[40] N. Ozpozan, H. Arslan, T. Ozpozan, M. Merdivan, N. Kulcu, J. Therm. Anal. Calorim. 61 (2000) 955–965.
[41] H. Arslan, O. Algul, Int. J. Mol. Sci. 8 (2007) 770–776.
[42] H. Arslan, D. Vanderveer, F. Emen, N. Kulcu, Z. Krist-New Cryst. St. 218 (2003) 479–480.
[43] C.K. Ozer, H. Arslan, D. VanDerveer, N. Kulcu, Molecules 14 (2009) 655–666.
[44] C.K. Ozer, H. Arslan, D. VanDerveer, G. Binzet, J. Coord. Chem. 62 (2009) 266–276.
[45] M. Gemili, Y. Nural, E. Keleş, B. Aydıner, N. Seferoğlu, E. Şahin, H. Sarı, Z. Seferoğlu, J. Mol. Liquids. 269 (2018) 920–932.
[46] O.V. Dolomanov, L.J. Bourhis, R.J. Gildea, J.A.K. Howard, H. Puschmann, J. Appl. Crystallogr. 42 (2009) 339–341.
[47] L. Palatinus, G. Chapuis, J. Appl. Crystallogr. 40 (2007) 786–790.
[48] L. Palatinus, A. van der Lee, J. Appl. Crystallogr. 41 (2008) 975–984.
[49] L. Palatinus, S.J. Prathapa, S. van Smaalen, J. Appl. Crystallogr. 45 (2012) 575–580.
[50] G.M. Sheldrick, Acta Crystallogr. C71 (2015) 3–8.
[51] A. Linden, Spek, Acta Crystallogr. C71 (2015) 9–18.